environments

MDPI

Article

Ecosystems in Mexico Are Experiencing an Increase in Trend and Intensity in Aridity

Leticia Citlaly López-Teloxa [1], Patricia Ruiz-García [2] and Alejandro Ismael Monterroso-Rivas [3,*]

[1] División de Ciencias Forestales, Universidad Autónoma Chapingo, Km 38.5 Carretera México-Texcoco, Texcoco 56230, Estado de México, Mexico; al2300036p@chapingo.mx
[2] Consultor Independiente, Calle Andador Primavera s/n, Col. Salitrería, Texcoco 56150, Estado de México, Mexico; patyrug31@gmail.com
[3] Departamento de Suelos, Universidad Autónoma Chapingo, Km 38.5 Carretera México-Texcoco, Texcoco 56230, Estado de México, Mexico
* Correspondence: aimrivas@correo.chapingo.mx; Tel.: +52-595-952-1500 (ext. 6178)

Abstract

This study examines the dynamics of aridity in Mexico in relation to El Niño–Southern Oscillation (ENSO) phases (El Niño, La Niña and neutral conditions) between 1999 and 2024. The aim is to identify ecosystems that are exposed to emerging aridification. Aridity was estimated using the Lang index at a resolution of 1 km across nearly two million grid cells. Aridity intensity and long-term trends were calculated and analysed by ENSO phase to identify areas of double exposure. Over 60% of Mexico is classified as arid or semi-arid. During El Niño, up to 100% of the central and southern regions exhibit increased aridity, affecting an area of 290,852 km^2 (14.7%), where both the intensity and the trend are high. Although La Niña typically brings wetter conditions, 150,022 km^2 (7.6%) still exhibit increasing aridity. Areas exposed to aridity under both ENSO phases cover 16,224 km^2 (0.8%), particularly affecting cloud forests, secondary vegetation and agricultural landscapes. This suggests a process of persistent aridification. The average arid area was 64% ± 7.51% during El Niño, 67% ± 1.44% during La Niña and 64% ± 8.14% during neutral years, indicating substantial variability beyond phase dependence. These findings reveal a complex, non-linear ENSO influence and suggest chronic hydroclimatic stress in some regions. Understanding which ecosystems experience recurrent aridity is crucial for effective water management, biodiversity conservation, and climate adaptation planning.

Keywords: lang index; climate anomalies; climate trends; double exposure; terrestrial ecosystems

Check for updates

Academic Editor: Joaquim Esteves Da Silva

Received: 25 February 2026
Revised: 19 March 2026
Accepted: 26 March 2026
Published: 28 March 2026

Copyright: © 2026 by the authors. Licensee MDPI, Basel, Switzerland. This article is an open access article distributed under the terms and conditions of the Creative Commons Attribution (CC BY) license.

1. Introduction

Aridity is a critical climatic condition characterised by a persistent shortage of water that affects terrestrial ecosystems [1]. This phenomenon manifests as reduced water availability, increased temperatures, and altered precipitation patterns, which impact soil microbiological processes and ecosystem [2,3]. Mexico is a country with a variety of climatic regions, so it is important to understand the spatial and temporal patterns of aridity in different terrestrial ecosystems to manage the environment effectively and implement strategies to adapt to climate change [4].

Mexico's terrestrial ecosystems are characterised by their exceptional biological diversity and ecological functionality [5]. They are important not only for the biodiversity they harbour, but also for the key functions they perform, such as carbon sequestration,

regulating the hydrological cycle and conserving soil [6,7]. However, the impact of aridity on these ecosystems has been reported with increasing frequency in recent years, raising concerns about their ecological integrity [8–10]. The most notable effects include changes in vegetation composition and structure, reduced primary productivity, biodiversity loss, altered ecosystem services, an increased risk of forest fires and changes in species' geographical distribution [11–13]. These impacts reflect the increasing pressure aridity is placing on the country's terrestrial ecosystems, highlighting the need for tools to monitor and predict such changes [14,15].

The El Niño-Southern Oscillation (ENSO) phenomenon can influence aridity in Mexico by altering precipitation and temperature patterns, thereby intensifying or mitigating aridity conditions [16,17]. ENSO is the primary interannual oscillation of the ocean–atmosphere system in the tropical Pacific and is characterised by alternating warm (El Niño), cold (La Niña) and neutral phases [18,19]. ENSO also significantly modifies sea surface temperature patterns and atmospheric circulation, generating teleconnections that affect regional and global climate [20]. ENSO can exacerbate or alleviate water stress in vulnerable ecosystems [21]. Therefore, integrated analyses are required to understand the compound risks to terrestrial ecosystems [22]. While this study does not focus on the direct impacts of ENSO, its different phases are considered to be drivers of the aridity conditions that will affect Mexico's terrestrial ecosystems.

In order to characterise aridity, tools capable of quantifying temporal and spatial variations are required [23]. Various climatic, hydroclimatic and ecohydrological indices have been used for this purpose, ranging in complexity from those that integrate only precipitation and temperature to those that also incorporate potential evapotranspiration, atmospheric balance, soil water storage and evaporative demand [24]. The most widely used climate indices include the UNEP Aridity index, which classifies humidity gradients based on precipitation and potential evapotranspiration [25]; the Martonne Index, which is based on the ratio of precipitation to average temperature [26]; the Standardised Precipitation Index (SPI), which focuses on precipitation anomalies and is useful for detecting droughts [27]; and the Standardised Precipitation Evapotranspiration Index (SPEI), which incorporates atmospheric evaporative demand and enables water deficits to be assessed over multiple time scales [28]. Indices such as the Palmer Drought Severity Index (PDSI) integrate ecohydrological processes by estimating soil water storage [29]. This diversity of tools reveals various aspects of water stress. However, for national-scale studies such as this one, it is particularly useful to employ simple and robust metrics based on widely recorded climate variables [30,31].

In this context, the Lang Index (LI) is a particularly suitable indicator because it reflects the relationship between precipitation and temperature directly, allowing for clear characterisation of climatic aridity gradients [32]. The LI provides a more detailed aridity classification and reduces the risk of underestimating arid conditions [33]. Furthermore, the LI has been widely applied in Mexico and is used as a reference in climate studies carried out by official institutions, such as the National Institute of Statistics and Geography (INEGI), which uses the modified Köppen classification for Mexico, developed by Enriqueta García, as its basis [34,35]. Similarly, the LI is employed to evaluate aridity in national studies, including those conducted for the National Atlas of Vulnerability to Climate Change [36]. Other indices have also been developed to date, such as the Standardised Precipitation Evapotranspiration Index (SPEI), which incorporates potential evapotranspiration (PET). However, applying it requires additional data on atmospheric evaporative demand and other variables. In contrast, temperature and precipitation indices, such as the Lang Index, are based solely on two widely available climate variables and have been shown to be useful for describing regional aridity gradients and vegetation patterns over large

areas [37,38]. Therefore, the LI is a suitable indicator for national scale analyses and long-term climate comparisons.

The LI provides valuable information on the water balance of terrestrial ecosystems by relating precipitation to temperature [31]. It allows aridity conditions to be quantified and facilitates the identification of areas under water stress [39]. The LI's simplicity and robustness as an indicator is based on its ability to integrate the two most decisive aridity-related climatic variables, precipitation and temperature, providing a comprehensive measure of the regional water balance [40]. Some authors claim that the LI shows less variation than Martonne, suggesting that it is more stable in the face of climatic fluctuations [41]. Analysing the intensity and trend of aridity patterns can reveal long-term changes, which is particularly relevant in the context of global climate change [42]. The objective of this study was therefore to identify the terrestrial ecosystems in Mexico that were most exposed to aridity between 1999 and 2024, by determining areas with double exposure (defined here as negative anomalies and a downward trend in the aridity index), based on the different phases of the ENSO phenomenon (El Niño, La Niña and Neutral). The hypothesis is that the El Niño phase increases drought in Mexico, and that this trend has become more pronounced in recent years. The results obtained contribute to our understanding of aridity patterns, which is crucial for developing effective strategies to maintain the ecological integrity and functionality of Mexico's terrestrial ecosystems in the face of ongoing climate change.

2. Materials and Methods

The methods are summarized in seven stages, as shown in Figure 1, and are described in more detail in the subsequent sections. (1) Delimitation of the study area, considering twelve precipitation influence zones and twenty terrestrial ecosystems; (2) Monthly temperature and precipitation data for the period 1999–2024, as well as the ONI classification of the ENSO phenomenon; (3) Estimation of the aridity index; (4) Calculation of the annual change in aridity intensity relative to the multi-year average; (5) Evaluation of aridity trends, focusing on magnitude (intensity), direction and spatial distribution; (6) Identification of statistically significant trends; (7) Analysis of double exposure to aridity in terrestrial ecosystems, based on aridity patterns observed in Mexican ecosystems. Steps 4 to 7 were carried out considering the ENSO phases to examine the influence of this climatic phenomenon on aridity patterns in different ecosystems. The study was conducted on a national scale, covering a 25-year time series (1999–2024) with pixel-level analysis and a spatial resolution of 1000 m. This equates to a total of 1,918,051 pixels. The procedures and tools used in each stage are described in detail below.

2.1. Study Area

The analysis was based on the country's classification into 12 precipitation influence zones, as previously defined in [43]. Each zone exhibits consistent rainfall patterns throughout the year. They are influenced by global and/or regional meteorological systems. The effect of local-level factors influencing rainfall, such as orography and energy balance, is also considered (see Supplementary Material S1). All of these factors are important for Mexico.

Land cover was considered using the most recent land use and vegetation map (Serie VII) [44] at a scale of 1:250,000. The cartography reports 183 variants of land use types in Mexico. However, for this study, these were grouped into 20 terrestrial ecosystem categories (Table 1), according to the most recent National Land Degradation Report [45], which emphasises aridity.

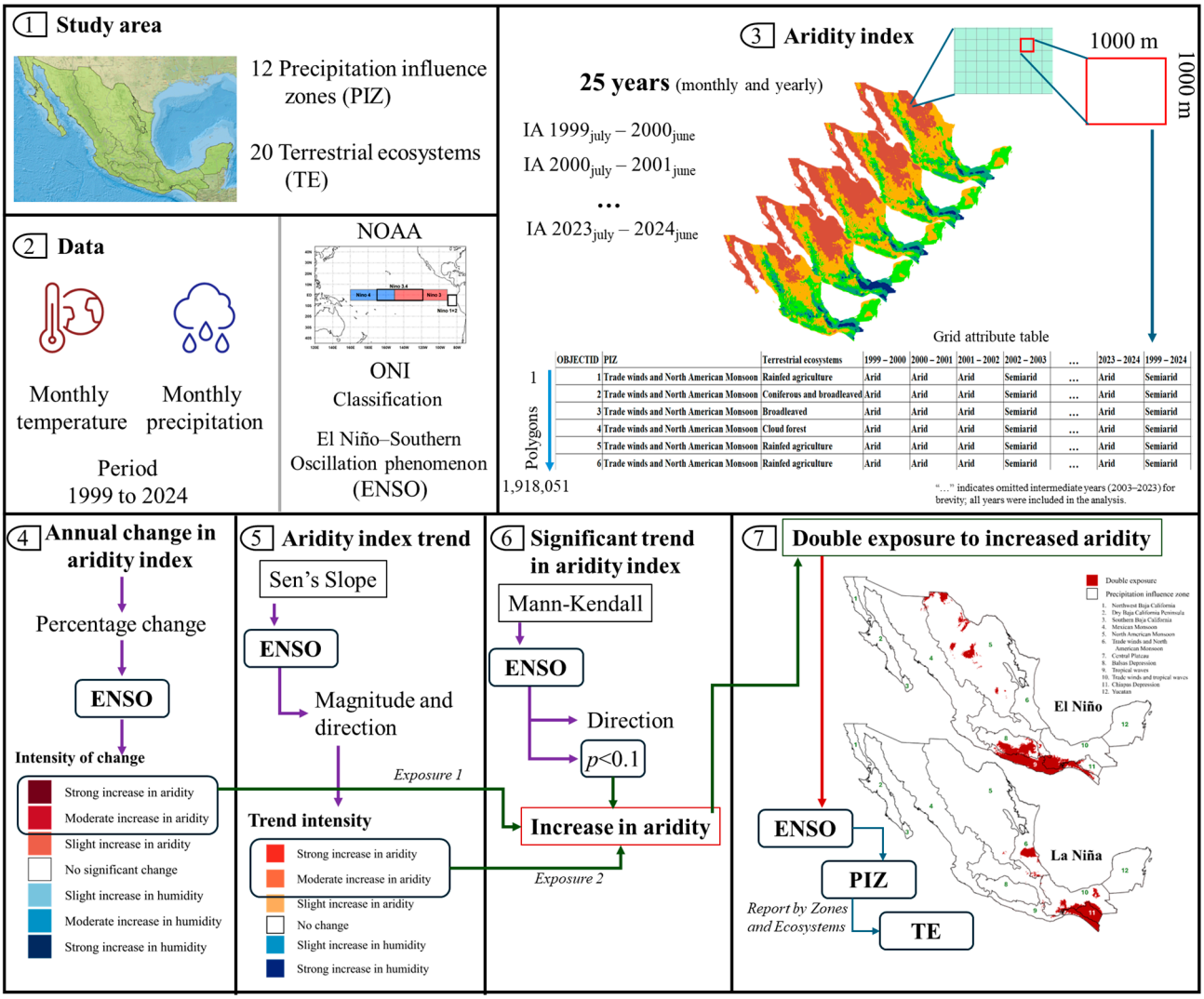


Figure 1. Flow chart showing how terrestrial ecosystems exposed to aridity in Mexico were identified for the period 1999–2024. (1) Study area, including 12 precipitation influence zones (PIZ) and 20 terrestrial ecosystems (TE); (2) Data sources: monthly temperature and precipitation (1999–2024) and ENSO classification based on the Oceanic Niño Index (ONI); (3) Aridity index calculation over 25 years (monthly and yearly), including grid resolution (1000 m) and attribute table structure (ellipses indicate omitted intermediate years for brevity); (4) Annual percentage change in aridity index and classification of change intensity; (5) Aridity index trend estimated using Sen's slope, indicating magnitude and direction of change; (6) Statistical significance of trends using the Mann–Kendall test ($p < 0.1$), identifying significant increases in aridity; (7) Double exposure to increased aridity associated with ENSO conditions (El Niño and La Niña), summarized by PIZ and TE.

Table 1. Classification of land use and vegetation in Mexico.

Land Use and Land Cover	Land System	Key
Wooded areas	Coniferous	CO
	Coniferous and broadleaved	CB
	Broadleaved	B
	Cloud forest	CF
	Highland and midland tropical forests	HMTF

Table 1. *Cont.*

Land Use and Land Cover	Land System	Key
Wooded areas	Lowland tropical forests	LTF
	Other wooded areas	OTHER
	Secondary forest vegetation	SFV
	Secondary rainforest vegetation	SRV
Grasslands and scrublands	Grasslands	G
	Arid scrubland	AS
	Semi-arid scrubland	SS
Coastal vegetation and mangroves	Coastal vegetation	CV
	Mangroves	MA
	Low floodplain vegetation	LFV
Agricultural areas	Rainfed agriculture	RA
	Irrigated agriculture	IA
Others	Human settlements	HS
	No apparent vegetation	NAV
	Water bodies	WB

Source: Prepared internally based on the INEGI Land Use and Vegetation Map Series VII [44].

2.2. Data

2.2.1. Temperature and Precipitation

Monthly minimum and maximum temperature data (in °C) and monthly and annual total precipitation data (in mm) were obtained from the WorldClim database [46]. The study period covers the years 1999 to 2024, with a spatial resolution of 2.5 min (approximately 21 km^2 at the equator). This period was chosen based on the availability and temporal consistency of the additional datasets required for the analysis, particularly those concerning land use and vegetation. Earlier climatic data were not incorporated as they do not correspond to the temporal coverage of these datasets, which could have resulted in inconsistent findings. The monthly database is a continuous series for the 25-year study period, guaranteeing the necessary temporal coverage for the analysis. This information formed the basis for estimating the monthly and annual value of the LI, enabling anomalies and trends to be analysed.

2.2.2. ENSO Data

Information was consulted from the National Oceanic and Atmospheric Administration (NOAA), based on the Oceanic Niño Index (ONI), which is available from the Climate Prediction Centre [47]. The ONI defines an event as occurring when sea surface temperature anomalies in the Niño 3.4 region persist for at least five consecutive quarters. This information was used to classify El Niño, La Niña and Neutral phases (Table 2). Various studies [18,48] have documented that ENSO events typically develop from July to December, reaching maximum intensity towards the end of the year before decaying in spring. Therefore, in this study, the beginning of each phase was considered to be in July, ending in June of the following year. Consequently, each hydrological year was associated with a Niño, Niña or Neutral phase, consistent with the aridity index.

Table 2. Bi-annual classification of ENSO phases: El Niño, La Niña, and Neutral.

Neutral	La Niña	El Niño
2001–2002, 2003–2004, 2012–2013, 2013–2014, 2019–2020	1999–2000, 2000–2001, 2005–2006, 2007–2008, 2008–2009 2010–2011, 2011–2012, 2016–2017, 2017–2018, 2020–2021, 2021–2022, 2022–2023	2002–2003, 2004–2005, 2006–2007, 2009–2010, 2014–2015, 2015–2016, 2018–2019, 2023–2024

Note: For each bi-annual year, July is the starting month and June the last month. Source: National Oceanic and Atmospheric Administration [47].

2.3. Aridity Index in Mexico

The LI is widely used in climate studies to characterise the degree of aridity in a region [31]. It is calculated as the ratio of total annual precipitation to average annual temperature. In our case, it is calculated over the period from July to June of the following year, as shown in Equation (1):

$$Lang\ index_{july1-june2} = \frac{\sum_{i=1}^{12} P_i}{\frac{1}{12}\sum_{i=1}^{12} T_i} \quad (1)$$

where i ranges from the month of July in year 1 to the month of June in year 2, P_i is the total precipitation for month i, expressed in millimetres (mm), and T_i is the average temperature for month i, expressed in degrees Celsius (°C). The aridity index is classified according to the intervals shown in Table 3.

Table 3. Classification of the aridity index according to Lang Index (LI) values.

Aridity Index	Level
IL $\leq$ 20	Arid
20 < IL$\leq$ 40	Semiarid
40 < IL $\leq$ 60	Subhumid
60 < IL $\leq$ 100	Humid
IL > 100	Per-humid

Source: Prepared internally based on [31,40].

The LI, which is used to classify aridity, does not assess the influence of ENSO. Rather, it was used to obtain an annual reference value, which was then associated with terrestrial ecosystems, as described below.

2.4. Intensity of Change in Aridity

Once aridity had been estimated, the rate of change continued to be estimated. An anomaly refers to the difference between the average aridity index for the entire study period (25 years) and the aridity index for each individual year. This procedure was carried out at pixel level by comparing the 25-year average for each pixel with the average for each individual year. This preserved the spatial detail in the estimation of anomalies. Each value was expressed as a percentage change in aridity anomaly (ΔAI) relative to the climatological average (the 25-year period), as defined in Equation (2) and applied to each year.

$$\Delta AI\ (\%) = \left(\frac{AI_i - \overline{AI})}{\overline{AI}} \right) \times 100 \quad (2)$$

where AI_i is the aridity index for year i, and $\overline{AI}$ is the 25-year average.

The anomaly in aridity change was therefore classified into seven ranges (Table 4), from an increase in humidity of more than 30% (i.e., a decrease in aridity) to an increase in aridity of more than 30%. In this context, "intensity" refers to the magnitude of the deviation from the 25-year climatological mean rather than an absolute physical measure. Thresholds were defined to represent progressively greater deviations from normal hydroclimatic conditions. This categorisation enabled the interannual spatial patterns of aridity change to be represented, facilitating their analysis in terms of the phases of the El Niño–Southern Oscillation (ENSO) phenomenon and their application to terrestrial ecosystems. Even moderate reductions in precipitation (10–20%) can substantially impact soil moisture, vegetation productivity, and water availability, especially in areas with limited water resources [49,50]. Therefore, percentage-based thresholds enable meaningful differentiation of hydroclimatic impacts.

Table 4. Intensity of change in the aridity index.

Range (%)	Intensity of Change
$\Delta AI \leq -30$	Strong increase in aridity
$-30 < \Delta AI \leq -15$	Moderate increase in aridity
$-15 < \Delta AI \leq -5$	Slight increase in aridity
$-5 < \Delta AI \leq 5$	No significant change
$5 < \Delta AI \leq 15$	Slight increase in humidity
$15 < \Delta AI \leq 30$	Moderate increase in humidity
$\Delta AI > 30$	Strong increase in humidity

Source: Authors' own elaboration.

It is important to note that a change in the aridity index implies a change in water availability. In terms of the absolute value of the aridity index (AI), a low value (e.g., 10) indicates arid conditions with less moisture available for vegetation and agriculture, while a higher value (e.g., 40) indicates wetter conditions with greater water availability for plants. Therefore, an increase or decrease in the anomaly (ΔAI) enables us to determine where and when a particular region has experienced drier or wetter conditions than normal, helping us to understand the impact of climate change on ecosystems and land use.

Once the intensity of the aridity change was obtained, it was correlated with ENSO. In other words, for each year and phase of El Niño, La Niña or Neutral (see Table 2), the corresponding aridity change intensity value was obtained. Thus, the corresponding ENSO phase, as well as the aridity value and aridity change intensity, was obtained for each pixel and for each of the 25 years. This provided the first indicator of exposure to aridity and made it possible to identify spatial patterns of increase or decrease in aridity associated with each ENSO phase. All processing was performed in the R programming environment using R Core Team [51].

2.5. Aridity Trend

To analyse trends in the aridity index, the time series (1999–2024) was divided into three phases according to the El Niño–Southern Oscillation (ENSO): El Niño, La Niña and neutral. This approach allowed the behaviour of aridity to be evaluated under distinct large-scale climatic conditions, rather than assuming a single, continuous temporal trend. As annual observations were grouped by ENSO phase, each subset consisted of relatively short, temporally discontinuous series representing specific climatic states.

The temporal evolution of the aridity index within each phase was assessed using Sen's non-parametric slope estimator (QSen), which is widely used in hydroclimatic studies due to its ability to withstand outliers and non-normal data distributions [52]. This method quantifies the magnitude and direction of monotonic trends by calculating the median

of all pairwise slopes in the time series. In this study, the estimator was applied on a pixel-by-pixel basis, converting the available observations for each phase into a single value representing the overall aridity trend.

A negative slope indicates a trend towards greater aridity (drier conditions), whereas a positive slope indicates a trend towards lower aridity (wetter conditions). A slope close to zero suggests that no clear linear trend was detectable during the analysed period. The resulting slopes were classified into six categories (see Table 5), ranging from strong increases in aridity to strong increases in humidity. These thresholds were defined to represent increasing magnitudes of change and facilitate interpretation of the spatial patterns of aridity trends across the study area.

Table 5. Trends in aridity according to aridity index values.

Range	Intensity of Change
QSen $\leq$ –1.0	Strong increase in aridity
–1.0 < QSen $\leq$ –0.5	Moderate increase in aridity
–0.5 < QSen $\leq$ –0.2	Slight increase in aridity
–0.2 < QSen $\leq$ 0.2	No significant change
0.2 < QSen $\leq$ 1.0	Slight increase in humidity
QSen > 1.0	Strong increase in humidity

Source: Authors' own elaboration.

Sen's slope is often used alongside the Mann–Kendall test, which evaluates the statistical significance of monotonic trends without requiring normally distributed data. However, serial autocorrelation may influence the performance of the Mann–Kendall test. In this study, the analysis was conducted on annual data subdivided by ENSO phase, producing short, temporally discontinuous series for each category. Under these conditions, reliable estimation of serial correlation is limited, and correction procedures may introduce additional uncertainty. Previous studies indicate that the influence of autocorrelation on Mann–Kendall results depends strongly on record length and persistence, and may be minor in annual hydroclimatic series with weak temporal dependence [53–55]. Therefore, the standard Mann–Kendall test was used to determine the statistical significance ($p < 0.1$) of the detected trends.

All processing was performed in the R programming environment using the R Core Team [51].

2.6. Assessment of Double Exposure to Aridity

The aridity intensity and trend results were analysed together and by ENSO phase. This is called double exposure to aridity. Double exposure was defined as the spatial overlap between areas with moderate or very strong annual change, and areas with statistically significant decreasing trends towards greater aridity (moderate or strong). This combination was correlated with a GIS land use and vegetation map to highlight regions where ecosystems face simultaneous climatic pressures, especially under different ENSO phases. This approach identified regions and ecosystems in Mexico that are most exposed to aridity, with a focus on the last 25 years.

2.7. Cartographic Data Processing and Analysis

To ensure spatial consistency in the analysis, a regular grid of 1000 m $\times$ 1000 m polygons was implemented across Mexico. This resulted in 1,918,051 spatial units. This grid provided a consistent spatial framework for combining variables from various sources with different original resolutions.

No resampling or downscaling of the climate datasets was performed. Instead, information was assigned to each grid cell based on its spatial correspondence. Climate variables derived from WorldClim, including the aridity index, as well as derived indicators such as intensity of change and aridity trends, were assigned to each polygon according to its location in Mexico. Similarly, thematic layers such as catchment areas and terrestrial ecosystems were intersected with the grid to assign the corresponding categorical attributes to each unit.

For continuous variables, values were assigned to each polygon based on its spatial overlap with the source data. This ensured a single representative value per unit while preserving the original spatial characteristics of the datasets. This procedure enabled the integration and comparison of environmental, climatic and spatial variables within a uniform analytical framework without altering their original resolution. The resulting grid provided a consistent basis for analysis at a national scale, facilitating the aggregation and standardisation of data across Mexico.

3. Results

3.1. Aridity Index and Terrestrial Ecosystems

Supplementary Material S2 presents aridity maps of Mexico from the last 25 years, and Figure 2 shows the average aridity index over this period. It can be seen that more than 60% of the country is arid or semi-arid (aridity index < 40). Aridity is concentrated in the northern, north-western, and central highland regions. By contrast, humid and semi-humid areas (aridity index > 60) are found along the Gulf of Mexico coast, in the Chiapas Depression and on the Yucatán Peninsula. These areas are influenced by trade winds, tropical waves and the North American monsoon [44].

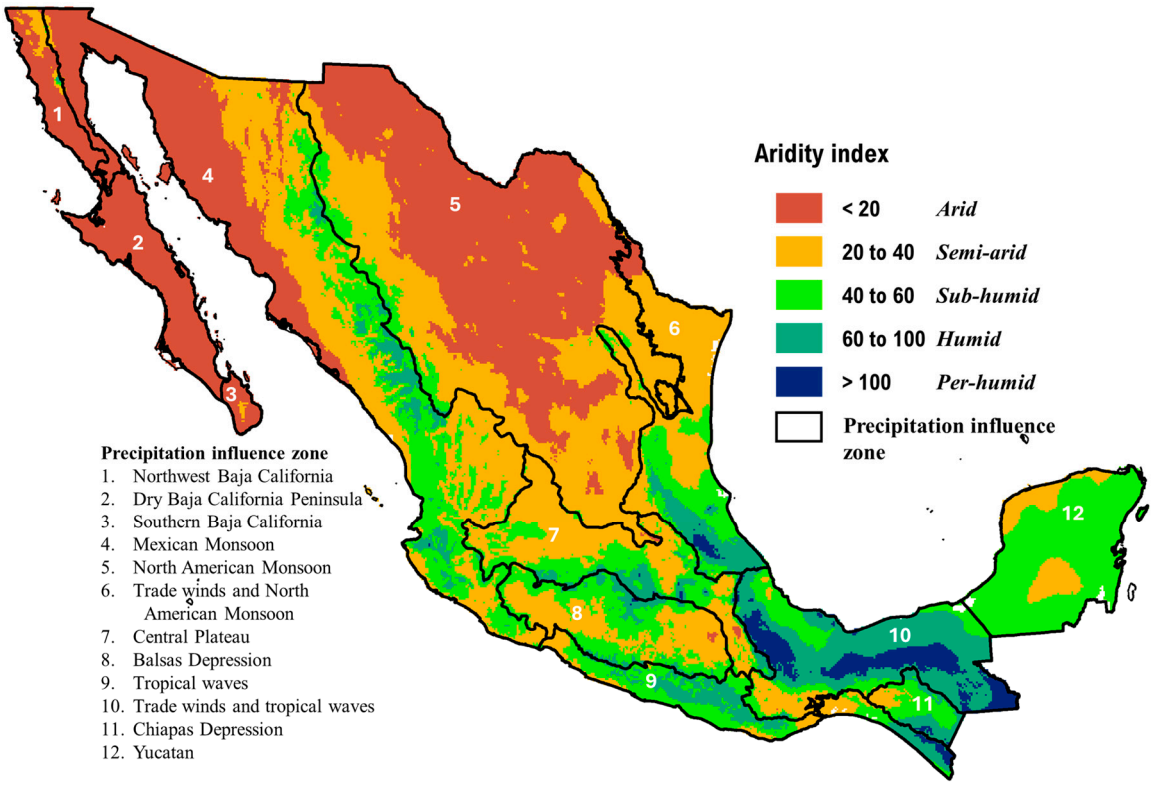


Figure 2. Spatial distribution of the average aridity index in Mexico between 1999 and 2024.

Arid and semi-arid regions are characterised by a high proportion of scrub ecosystems and agricultural areas. By contrast, humid and semi-humid areas support greater

structural and functional diversity, particularly in tropical rainforests and cloud forests (see Supplementary Material S3). Examining the behaviour of annual aridity in detail according to land use type reveals significant differences (Figure 3). For instance, in the precipitation region known as the Dry Baja California Peninsula, virtually all land uses over the past 25 years have had an aridity index identifying them as arid (less than 20). Another region that stands out for having no apparent changes in aridity is the Yucatan Peninsula, where the subhumid category predominates and this condition appears to have remained unchanged throughout the study period.

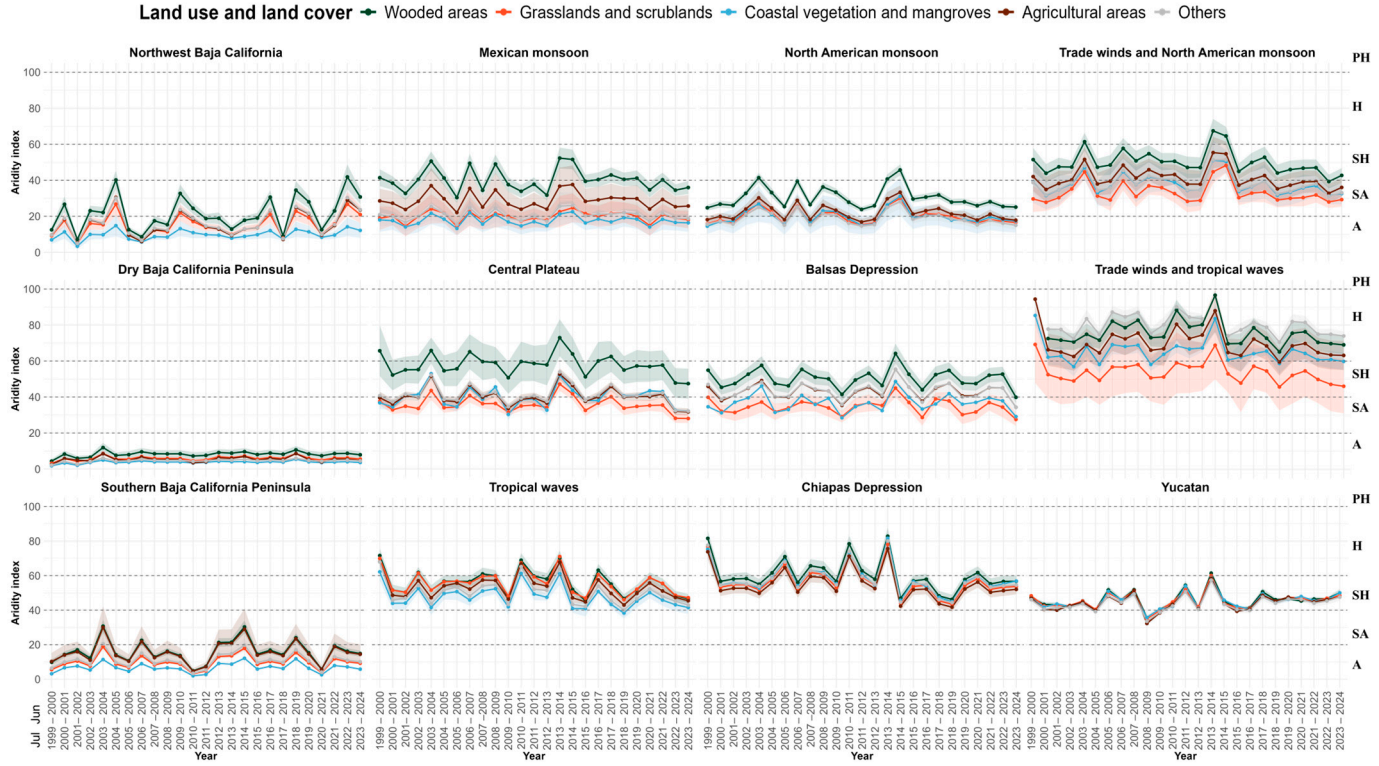


Figure 3. Average aridity index (1999–2024) by precipitation zone and land use. Where A = arid, SA = semi-arid, SH = sub-humid, H = humid, PH = perhumid.

In the Mexican monsoon region, the North American monsoon region, the Central Plateau and the Balsas Depression, aridity index values mainly fluctuate between 20 and 60, corresponding to semi-arid and subhumid conditions. In these areas, forest ecosystems have maintained average conditions; however, the last ten years (since 2014) have seen a sustained increase in aridity, as evidenced by a progressive reduction in index values. Since 2014, a shift towards lower humidity levels has been observed in the Chiapas Depression in the south of the country, where peaks or increases in humidity were no longer observed. See Supplementary Material S4 for a detailed analysis of the aridity index in the 12 regions considered.

3.2. Intensity of Aridity Change

Figure 4 illustrates the variation in the intensity of changes to the aridity index, expressed as a percentage of the national territory experiencing increases in aridity or humidity, in relation to the phases of the ENSO phenomenon between 1999 and 2024. Throughout the analysed period, notable interannual variability is evident in the spatial distribution of changes to the Aridity index, with some years showing changes in more than 80% of the national territory (see Supplementary Material S5). This suggests a nonlinear response of the regional climate system to ENSO phases, i.e., positive or negative variations

in sea surface temperature relative to the climatological average. Generally, during years associated with El Niño events (marked in red), a larger proportion of the surface area experienced moderate to strong increases in aridity. Conversely, years dominated by La Niña conditions (marked in blue) showed a higher percentage of territory with slight or moderate increases in humidity, reflecting a reduction in aridity. However, there were exceptions to this general pattern. For instance, in certain El Niño years (e.g., 2006–2007 and 2014–2015), the proportion of land experiencing moderate or severe increases in aridity was relatively low. Conversely, in some La Niña years (e.g., 2020–2021 and 2022–2023), the increase in wet conditions was limited. These results demonstrate that the spatial response of aridity to ENSO phases is not consistent.

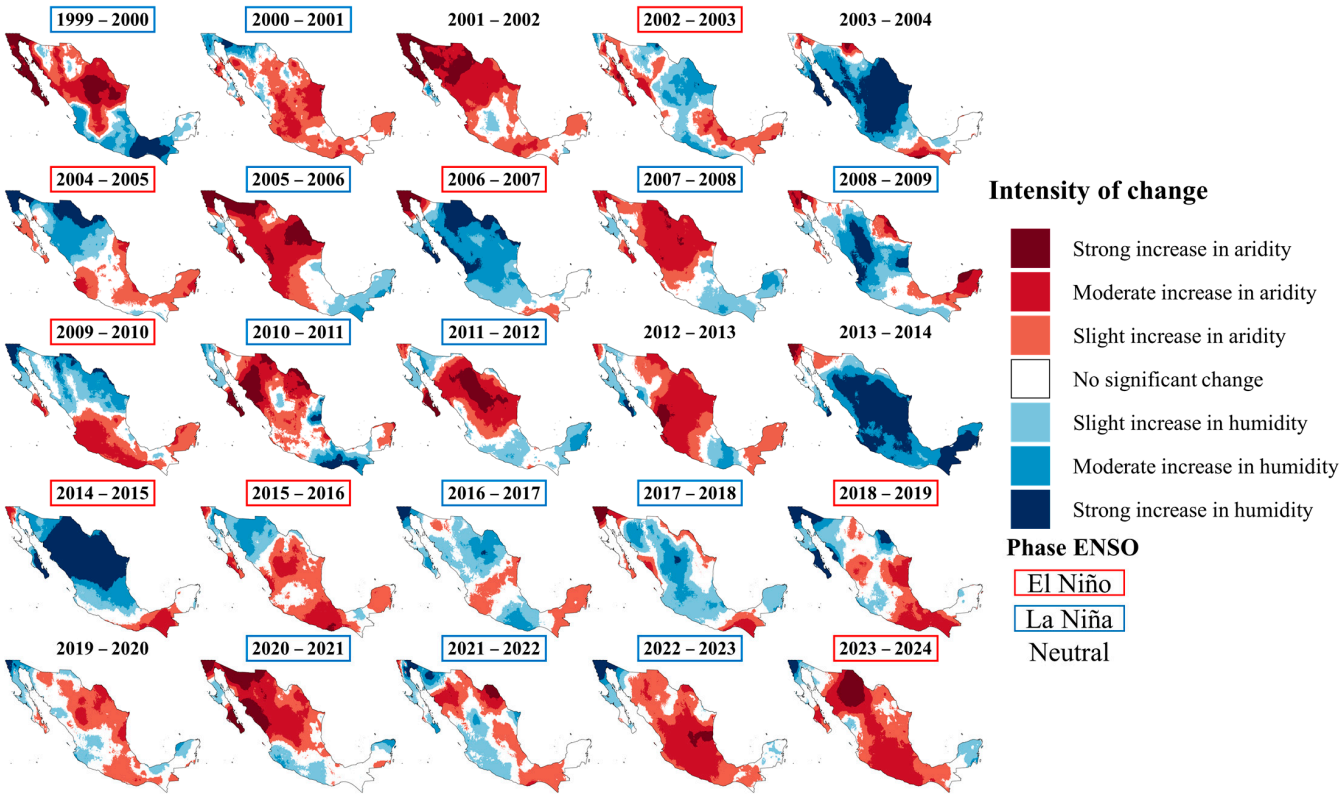


Figure 4. Annual intensity of change in the aridity index according to occupied surface area by country.

The years 2015–2016 and 2023–2024 stand out as significant periods during which a large proportion of the national territory experienced increases in aridity, both being El Niño phases. In fact, more than 60% of the total area experienced arid conditions, reflecting much drier conditions. By contrast, during the years associated with La Niña events (2007–2008, 2008–2009, 2010–2011 and 2017–2018), a larger area experienced relatively wetter conditions.

Notably, in several years, a significant proportion of the national territory (up to 40%) showed no significant changes in the index value, suggesting stability in local conditions despite the influence of global climatic phenomena. However, this stability varies markedly between years, indicating that aridity is highly sensitive to ENSO phases on a spatial and temporal scale.

Table 6 summarises the occupied surface area according to ENSO phase and moderate to severe aridity index. In the Baja California peninsula (taking into account its three climatic regions: North-western Baja California, the Dry Peninsula of Baja California, and the Southern Peninsula of Baja California), the area affected by increased aridity is generally high, although there are clear differences between subregions and climatic phases.

La Niña tends to concentrate the largest proportion of the impacted area throughout the peninsula, while El Niño significantly reduces this area in the driest northern and central regions. The southern region of the peninsula is the most sensitive to interannual variability, showing a clear dependence on ENSO phases for increases in aridity, particularly under cold conditions.

Table 6. National area according to aridity intensity and trend (moderate and severe), and precipitation influence zone according to ENSO phase.

Precipitation Influence Zone	Intensity			Trend		
	Neutral	El Niño	La Niña	Neutral	El Niño	La Niña
	Percentage of Surface (%)					
Northwest Baja California	100.0	97.1	100.0	0.0	0.0	0.0
Dry Baja California Peninsula	63.6	41.3	100.0	25.8	0.0	0.0
Southern Baja California Peninsula	0.0	51.3	100.0	98.7	0.0	0.0
Mexican monsoon	99.8	62.4	99.3	5.4	37.6	0.1
North American monsoon	97.4	70.8	100.0	13.6	78.0	0.0
Trade winds and North American monsoon	55.9	76.7	100.0	33.2	79.5	45.8
Central Plateau	44.1	99.9	96.3	42.9	74.3	11.4
Balsas Depression	29.3	100.0	99.9	4.4	94.0	3.0
Tropical waves	56.6	100.0	77.3	0.0	100.0	57.2
Trade winds and tropical waves	23.7	90.3	22.5	10.1	43.9	98.0
Chiapas Depression	8.7	100.0	100.0	0.0	81.9	100.0
Yucatán	0.3	29.0	89.2	0.6	0.0	4.3

Note: the percentages are not additive and should not total 100%. Intensity and aridity trends were analysed independently for each climate phase (Neutral, El Niño and La Niña).

3.3. Temporal Trend in Aridity

Figure 5 shows the spatial distribution of aridity trends during the different phases of the ENSO phenomenon (El Niño, La Niña and neutral conditions). Red tones indicate an increase in aridity, while blue tones represent a decrease, or wetter conditions. El Niño events generally promote a widespread increase in aridity across much of the country (see Supplementary Material S7). Conversely, La Niña phases are associated with a decrease in aridity in large regions of northern and western Mexico, which coincides with monsoon systems and areas influenced by trade winds.

Table 6 shows the percentage of the area within each precipitation zone that experiences increasing (moderate or strong) aridity trends, separated by ENSO phase.

3.4. Double Exposure to Aridity

Figure 6 illustrates regions experiencing significant double exposure to aridity, which is defined as areas where both aridity intensity and increasing aridity trends are present. This refers to regions where joint analysis of Sen's slope and Mann–Kendall was statistically significant ($p < 0.1$). The red areas represent critical zones due to double exposure to aridity, depending on whether it is an El Niño or La Niña phase.

During El Niño years, the combination of aridity intensity and trend affects 290,852 km^2 nationwide (14.7%). In contrast, during La Niña years, the area affected by intensity and trend was 150,022 km^2 (7.6%). During years with neutral conditions, no areas with significant double exposure were identified. Notably, 16,224 km^2 of national territory (0.8%) experienced continuous aridity due to a succession of La Niña phases followed by El Niño phases. This suggests sustained aridification regardless of ENSO phase changes. The most affected ecosystems in this area were recovering vegetation (49% of its area), mesophilic mountain forest (25%), and agriculture (20%). For more information, see Supplementary Material S7, S8 and S9.

During the El Niño phase, the largest area of double exposure was concentrated in the Tropical Waves region, where all land uses exhibited high values. In this region, the largest exposed areas were found in coniferous forests (85%) and in mixed coniferous and broadleaved forests (88%). By contrast, the Balsas Depression exhibited moderate values, with a larger exposed area in wooded areas; cloud forest accounted for 48% of this. Although the Central Plateau had the lowest percentage of exposed surface area of all the analysed regions, its wooded areas, which are mainly coniferous and broadleaved forests, accounted for the highest percentage of exposed surface area at 9%.

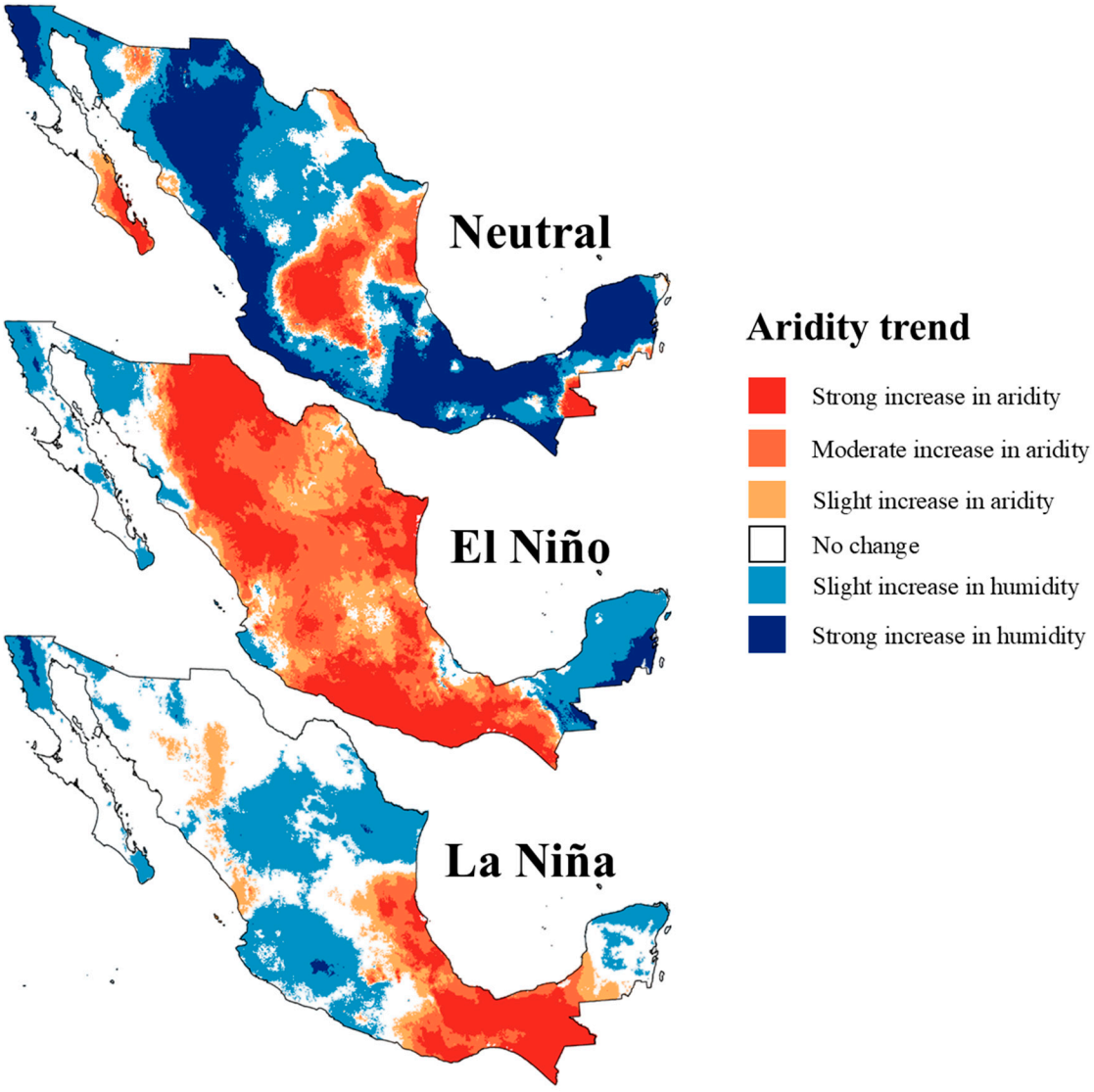


Figure 5. Trends in changes to the aridity index according to ENSO phase over the last 25 years (1999–2024).

During the La Niña phase, exposure reached its maximum value in the Chiapas Depression, where all land cover types had a 100% exposed surface area. In contrast, regions such as Trade Winds and North American Monsoon and Trade Winds and Tropical Waves showed moderate and relatively homogeneous exposure across coverage types. In these regions, the terrestrial ecosystems with the largest exposed surface areas were mangroves (70%) and coniferous and broadleaved forests (30%), respectively. In the region associated with tropical waves, exposure decreased compared to the El Niño phase. However, a clear pattern emerged, with coastal vegetation and mangroves having the

highest exposure rates within the region (80% of the area), surpassing forests, grasslands and agricultural areas.

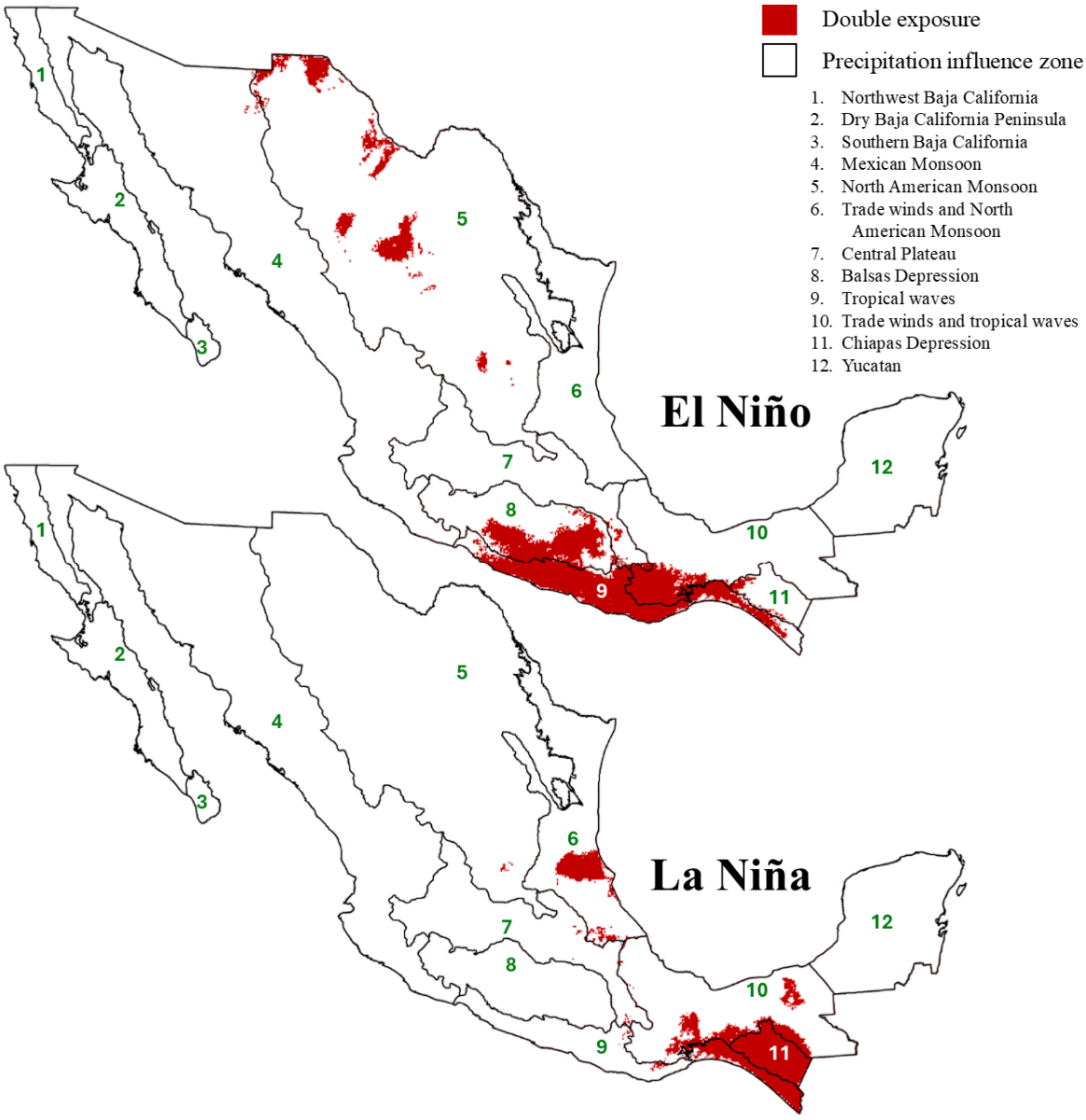


Figure 6. Regions with double exposure to aridity (in terms of both intensity and trend areas with Sen's slope and Mann–Kendall statistically significant ($p < 0.1$)) by ENSO phase over the last 25 years.

Table 7 shows the aridity trend by precipitation region. During the El Niño phase, aridity increased at an average rate of −10.83 units per year. During La Niña, however, the increase was more pronounced at −18.08 units per year. The Tropical Waves region experienced a significant increase in aridity during both the El Niño and La Niña phases. The annual increase in aridity was more pronounced in the Tropical Waves and Trade Winds and North American Monsoon regions during the La Niña phase. It is important to note that these trends were calculated for areas identified as having significant dual exposure to aridity only. Consequently, negative Sen slopes are expected across all regions, as the analysis focuses exclusively on areas already experiencing intensifying arid conditions.

Table 7. Trends in aridity by precipitation influence zone during El Niño and La Niña phases.

Precipitation Influence Zone	El Niño	La Niña
Tropical waves	−14.01	−33.35
North American monsoon	−4.03	−0.13
Trade winds and North American monsoon	ND	−26.68
Mexican monsoon	−2.60	ND
Trade winds and tropical waves	−1.71	−7.77
Balsas Depression	−1.40	−0.56
Central Plateau	−1.26	−1.12
Chiapas Depression	−0.95	−5.74
Annual Mean	−10.83	−18.08

Note: the values represent the regional average Sen slope (Q_(Sen)), which is obtained from pixel-by-pixel estimates and filtered by statistical significance (Mann–Kendall test, $p < 0.1$) for each precipitation influence zone. Negative values indicate an increasing trend towards aridity. These trends were calculated for areas with significant dual exposure to aridity only (see text), which explains the consistently negative values. ND = No data.

4. Discussion

This study identified the terrestrial ecosystems that are most exposed to increasing aridity, which is derived from variability associated with ENSO phases. The implications of these results are discussed below in relation to the aridity index, the intensity of change, temporal trends and double exposure in different terrestrial ecosystems.

4.1. Aridity in the Period 1999–2024

Aridity in Mexico has increased significantly over the last 25 years, as reflected by the variation in the area experiencing arid conditions. According to [56], approximately 61% of the national territory was arid in 2002. Fifteen years later, the [57] reported this figure had increased to 65%. The present study found that 66% of the national territory is now arid. This is consistent with the findings reported in [58], who estimated that approximately 66.5% of Mexico is arid.

The arid conditions in Mexico are caused by dry air masses descending from Hadley cells in the atmosphere, generating high-pressure belts in the north of the country [59]. The terrain also plays a role, with the mountains creating a rain shadow effect that prevents moisture from reaching the Altiplano [60]. Similarly, cold ocean currents in the Pacific stabilise the atmosphere, limiting precipitation in the northwest and intensifying these dry conditions [61].

4.2. Aridity and ENSO

The results show that the aridity index varies according to ENSO phases and across different regions of the country and different precipitation zones. This is due to the strong correlation between ENSO phases and the regional climate regime [62]. While El Niño events amplify aridity in the centre and south of the country, La Niña phases tend to reverse these effects to some extent, favouring wetter conditions in tropical and monsoon regions [63]. This behaviour is replicated throughout Central America and northern South America [64], where it was observed that La Niña increased precipitation in the Amazon basin compared to the neutral period; however, the opposite occurred during El Niño events.

However, while the results confirm an association between ENSO phases and changes in the Aridity Index, the responses demonstrate significant interannual variability rather than a straightforward phase-dependent pattern. On average, the arid area was 64% ± 7.51% during El Niño years, 67% ± 1.44% during La Niña years, and 64% ± 8.14% during neutral years. While the mean value is slightly higher during La Niña years, the much greater variability during El Niño years suggests that some El Niño events result

in more extensive arid conditions than those observed during La Niña years. This emphasises the episodic and spatially heterogeneous nature of ENSO's impact on Mexico, where regional climatic factors and land-atmosphere interactions can influence the expected hydroclimatic response. Therefore, the results suggest a complex, nonlinear relationship between ENSO phases and aridity rather than a systematic inverse relationship between El Niño and La Niña conditions.

Furthermore, the magnitude of changes in aridity depends not only on the ENSO phase, but also on the intensity of each event and how it interacts with regional atmospheric conditions. Some years classified as El Niño or La Niña showed relatively weak responses in terms of the extent to which the landscape became drier or wetter, suggesting that moderate or weak events may not generate climate anomalies intense enough to produce widespread impacts on the landscape. This behaviour is consistent with studies indicating that the hydroclimatic response in Mexico depends heavily on the intensity of ENSO and its interaction with other modes of climate variability. This results in non-linear, regionally differentiated spatial patterns [65–67].

Moderate to intense decreases in aridity were observed in the northwestern regions of the Baja California Peninsula, the Mexican Monsoon region and the North American Monsoon region during neutral phases (39%, 24% and 34% respectively). This coincides with observations reported in [68], who note that during neutral ENSO phases, variability in extreme precipitation events increases in northwestern Mexico, including areas of Baja California. During these periods, precipitation may decrease in quantity or intensity, and there may be greater atmospheric variability due to the reduced direct influence of oceanic–atmospheric phenomena associated with ENSO and its extreme phases (El Niño or La Niña). Furthermore, drier conditions in northwestern Mexico tend to occur during neutral years. This suggests that internal atmospheric factors, such as the variability of the North Pacific Subtropical High, also play a key role in modulating regional dry conditions [69]

This behaviour suggests that the variability of the Aridity index in these areas may be influenced by climatic factors other than ENSO. These factors include the Arctic Oscillation (AO), the Madden–Julian Oscillation (MJO) and regional circulation patterns, such as the North Pacific subtropical anticyclone. These factors can affect the distribution of humidity and temperature, even in the absence of thermal anomalies in the equatorial Pacific. Although ENSO events are predominant, they do not fully explain the variability of precipitation and temperature in regions north of Mexico [70]. Other atmospheric forcings and circulation modes also play an important role. Additionally, topography, continentality and intraseasonal variability could amplify the local effects of smaller-scale atmospheric events, rendering certain regions more susceptible to changes unrelated to El Niño or La Niña. For instance, the MJO influences summer rainfall variability and moisture fluxes in Mexico, suggesting that seasonal and intraseasonal variability can impact water availability independently of ENSO anomalies [71].

4.3. Ecosystems and Exposure to Aridity

This study found that during El Niño years, arid areas expand in the north of the country. In contrast, the central region experiences an increase in humid areas, while humid areas decrease in the south. By contrast, during La Niña years, arid areas expand in the north and centre of the country, while humid areas increase in the south. Under neutral ENSO conditions, no homogeneous spatial trend was identified at the national level, although a relative increase in arid areas was observed. These results are partially consistent with those reported in [59], which found that during El Niño events, precipitation increased in northern and northwestern Mexico and decreased in the south. During La Niña events,

they found an increase in precipitation in the south and a decrease towards the north, with no significant changes in the central region under neutral conditions.

These changes in moisture distribution generate variations in water availability and productivity in different ecosystems and land uses, affecting their vulnerability to ENSO events.

In forest ecosystems such as coniferous forests, cloud forests and tropical rainforests, double exposure is primarily concentrated in the Chiapas Depression and tropical waves, and to a lesser extent in the Balsas Depression. These regions are characterised by high biological productivity and play a key role in the carbon cycle [60]. A trend towards drier conditions in these ecosystems could lead to reduced soil moisture and carbon sequestration capacity, impacting soil respiration dynamics and natural regeneration processes [1,13].

In cloud forests, where climatic stability depends on the balance between precipitation and cloud cover, a sustained decrease in the aridity index could result in a loss of humid microclimates, which would have consequences for endemic species and local water recharge processes. This is consistent with the findings reported in [72], which demonstrated that increased aridity alters productivity thresholds and generates feedback loops of ecological degradation in humid tropical regions.

Agricultural areas, particularly rain-fed areas, are highly susceptible to increases in aridity. Significant downward trends in the Aridity index during El Niño events suggest a decrease in water availability for crops, potentially leading to yield losses and increased vulnerability to agricultural droughts [72,73]. Furthermore, adjusting sowing dates in line with ENSO phases, for example by sowing later during El Niño and earlier during La Niña, can improve yields and reduce variability in yields [74]. In irrigation systems, pressure on groundwater resources could intensify and exacerbate imbalances in areas that are already overexploited. This scenario coincides with reports of changes in rainfall seasonality and higher temperatures under positive ENSO conditions [68,75].

In arid and semi-arid systems, particularly in the north and north-west of the country, exposure to aridity is doubly critical. This is because the Aridity index is in the <40 range due to its characteristics, and because declines in this index occur frequently during El Niño events. These areas correspond to desert scrub and grassland ecosystems, which already operate close to the functional thresholds of water availability [69]. The loss of vegetation cover and the degradation of soil organic carbon can intensify desertification processes, reducing the capacity to retain water and nutrients [76]. This behaviour is consistent with the "aridisation tipping points" model proposed in [1]. According to this model, dry ecosystems respond non-linearly to increases in water stress, which can trigger abrupt losses of functionality.

Although coastal areas and wetlands occupy only a small proportion of the national territory, they play a fundamental role in the hydrological cycle. Regions such as the coastal plains of the Gulf and the southern Pacific are at risk of alterations in freshwater flows and salinity due to double exposure to decreases in the aridity index and moderate aridity trends, which has implications for mangroves and floodplain vegetation [77,78]. This risk is reportedly amplified by the effects of the positive ENSO phase, which increases the frequency of droughts by reducing summer rainfall across the country and restricting the flow of tropical maritime air to the Pacific coast by strengthening the trade winds [63]. A decrease in continental water inputs during El Niño events has been identified as a key factor in mangrove biomass loss and changes to the flora of coastal wetlands [79].

These findings emphasise the importance of considering multiple climate forcings when analysing the dynamics of the Aridity index, particularly in regions with significant internal variability. They also emphasise the necessity of conducting further regional studies that integrate atmospheric variables with greater temporal and spatial resolution,

with the aim of improving our understanding of the mechanisms controlling the response of ecosystems and local climate beyond the influence of ENSO.

The results show that increased aridity, particularly during El Niño events, affects Mexico's ecosystems in different ways and can have negative impacts on terrestrial systems [68]. Identifying areas with significant double exposure indicates that climate impacts are not only transient, but also reflect the intensification of aridity processes. These transformations compromise the stability of ecosystem services, biological productivity and socio-environmental resilience in various systems throughout the country [80].

5. Conclusions

In addition to naturally arid ecosystems, ecosystems exposed to aridity were identified. The results confirm that El Niño and La Niña phases have contrasting and spatially heterogeneous effects on aridity in different regions of Mexico, with no evidence of one phase having a systematically greater impact than the other. However, some El Niño events do lead to more extensive expansions of arid conditions. Evidence of increasing aridity also began to emerge during the La Niña phase. Identifying areas with double exposure highlights regions that are particularly vulnerable to climate change, where increased aridity may persist and continue during the neutral phase. Overall, the country is experiencing changes towards greater aridification. These findings provide insight into how variations in precipitation and temperature, influenced by ENSO, translate into patterns of drought and water resource availability across the country. As some ecosystems are exposed, future research may focus on monitoring evidence of drought stress and aridity. This information could inform water management policies and adaptation strategies in regions with double exposure. However, the analysis is limited by the spatial resolution and use of a single aridity index. Using other drought indicators, such as the Standardised Precipitation Index (SPI) or the Standardised Precipitation Evapotranspiration Index (SPEI), which take into account precipitation or evapotranspiration anomalies, could lead to different interpretations of hydroclimatic dynamics. Nevertheless, the results consistently indicate an increasing trend towards aridity across the country. Furthermore, future studies should explore the interaction between different climatic phenomena in greater depth, as well as assess the effectiveness of mitigation measures in areas identified as highly vulnerable. Furthermore, future studies should examine how different climatic phenomena interact with each other and evaluate the effectiveness of mitigation measures in areas that have been identified as being highly vulnerable.

Supplementary Materials: The following supporting information can be downloaded at: https://www.mdpi.com/article/10.3390/environments13040187/s1, Supplementary Material S1: Terrestrial ecosystems and main precipitation influence zones. Supplementary Material S2: Annual aridity index. Supplementary Material S3: Area (km^2) by climate region and land system. Supplementary Material S4: Annual aridity index in the 12 zones of precipitation influence and dominant terrestrial ecosystems. Supplementary Material S5: Interannual spatial variation in change intensity. Supplementary Material S6: Area (in km^2) with moderate and strong increases in aridity change intensity, by precipitation influence zone, terrestrial ecosystem and phase. Supplementary Material S7: Area (km^2) with moderate and strong increase in aridity trend intensity by precipitation influence zone, terrestrial ecosystem and phase. Supplementary Material S8: Area in km^2 with significant double exposure by precipitation influence zone and terrestrial ecosystem in the El Niño phase. Supplementary Material S9: Area (km^2) with significant double exposure by precipitation influence zone and terrestrial ecosystem in La Niña phase.

Author Contributions: Conceptualization, L.C.L.-T., P.R.-G. and A.I.M.-R.; Methodology, L.C.L.-T., P.R.-G. and A.I.M.-R.; Software, L.C.L.-T.; Validation, L.C.L.-T., P.R.-G. and A.I.M.-R.; Formal analysis, L.C.L.-T., P.R.-G. and A.I.M.-R.; Investigation, L.C.L.-T.; Data curation, L.C.L.-T.; Writing—original

draft preparation, L.C.L.-T., P.R.-G. and A.I.M.-R.; Writing—review and editing, L.C.L.-T., P.R.-G. and A.I.M.-R.; Visualization, L.C.L.-T.; Supervision, A.I.M.-R. All authors have read and agreed to the published version of the manuscript.

Funding: This research received no external funding. Dr. Lopez receives financial support from the Secretaría de Ciencia, Humanidades, Tecnología e Innovación (SECIHTI) for her postdoctoral stay in the Postgraduate Programme in Forestry and Environmental Sciences at Universidad Autonoma Chapingo.

Data Availability Statement: Data are available upon reasonable request from the corresponding author.

Acknowledgments: SECIHTI for financial support, DGIP, CIRENAM and the Department of Forest Sciences of Universidad Autonoma Chapingo. To the anonymous reviewers.

Conflicts of Interest: The authors declare no conflicts of interest.

References

1. Berdugo, M.; Delgado-Baquerizo, M.; Soliveres, S.; Hernández-Clemente, R.; Zhao, Y.; Gaitán, J.J.; Gross, N.; Saiz, H.; Maire, V.; Lehmann, A.; et al. Global Ecosystem Thresholds Driven by Aridity. *Science* **2020**, *367*, 787–790. [CrossRef] [PubMed]
2. Huang, J.; Yu, H.; Guan, X.; Wang, G.; Guo, R. Accelerated Dryland Expansion under Climate Change. *Nat. Clim. Change* **2016**, *6*, 166–171. [CrossRef]
3. Ortega-Gaucin, D.; Bartolón, J.D.l.C.; Bahena, H.V.C. Drought Vulnerability Indices in Mexico. *Water* **2018**, *10*, 1671. [CrossRef]
4. Seingier, G.; Jiménez-Orocio, O.; Espejel, I. Vulnerability to the Effects of Climate Change: Future Aridness and Present Governance in the Coastal Municipalities of Mexico. In *Stewardship of Future Drylands and Climate Change in the Global South: Challenges and Opportunities for the Agenda 2030*; Lucatello, S., Huber-Sannwald, E., Espejel, I., Martínez-Tagüeña, N., Eds.; Springer International Publishing: Cham, Switzerland, 2020; pp. 301–320.
5. Barreras, A.; de la Rosa, J.A.A.; Mayorga, R.; Cuenca, R.; Moreno-G, C.; Godínez, C.; Delgado, C.; Soriano-Luna, M.d.L.Á.; George, S.; Aldrete-Leal, M.I.; et al. Spatial Predictions of Tree Density and Tree Height across Mexico Forests Using Ensemble Learning and Forest Inventory Data. *Ecol. Evol.* **2023**, *13*, 10090. [CrossRef]
6. Solano, A.L.; Martínez, D.; Corral, L.; Sánchez, G. Tendencias Ecológicas y Socioeconómicas de Los de Pino-Encino En Centroamérica: Aportes Para Su Manejo. *Rev. Mesoam. Biodivers. Y Cambio Climático* **2017**, *2*, 38–47.
7. Fernández, A.S.; Cabrera, I.I.V.; Ruiz, L.M.P.; Ávila, E.C.; Cobos, F.A.; Ortega, J.B. Resilience of Vegetation Cover in Southwest Mexico to the Climate Change Effects. *Rev. Peru. Biol.* **2021**, *28*, 18187. [CrossRef]
8. Speich, M.J.R. Quantifying and Modeling Water Availability in Temperate Forests: A Review of Drought and Aridity Indices. *IForest* **2019**, *12*, 1–16. [CrossRef]
9. Klaus, J.; Monk, W.A.; Zhang, L.; Hannah, D.M. Ecohydrological Interactions during Drought. *Ecohydrology* **2022**, *15*, e2456. [CrossRef]
10. Yin, L.; Wang, Y.; Sun, C.; Ye, Y. Spatiotemporal Evolution and Risk Analysis of Land Use in the Coastal Zone of the Yangtze River Delta Region of China. *Remote Sens.* **2023**, *15*, 2261. [CrossRef]
11. Quintana, J.R.; Martín-Sanz, J.P.; Valverde-Asenjo, I.; Molina, J.A. Drought Differently Destabilizes Soil Structure in a Chronosequence of Abandoned Agricultural Lands. *Catena* **2023**, *222*, 106871. [CrossRef]
12. Werner, C. Extreme Droughts and Heatwaves Endanger Temperate Forests. *Plant Biol.* **2022**, *24*, 1091–1092. [CrossRef]
13. Correa-Díaz, A.; Villanueva-Díaz, J.; Gómez-Guerrero, A.; Martínez-Bautista, H.; Castruita-Esparza, L.U.; Horwath, W.R.; Silva, L.C.R. A Comprehensive Resilience Assessment of Mexican Tree Species and Their Relationship with Drought Events over the Last Century. *Glob. Change Biol.* **2023**, *29*, 3652–3666. [CrossRef]
14. Werner, C.; Haberstroh, S.; Seifert, T.; Christen, A.; Caldeira, M. Impacts of Severe Droughts on Species Interaction in Forests. In Proceedings of the EGU General Assembly Conference Abstracts, Vienna, Austria, 23–28 April 2023; p. EGU-9525.
15. Bendall, E.R.; Bedward, M.; Boer, M.; Clarke, H.; Collins, L.; Leigh, A.; Bradstock, R.A. Changes in the Resilience of Resprouting Juvenile Tree Populations in Temperate Forests Due to Coupled Severe Drought and Fire. *Plant Ecol.* **2022**, *223*, 907–923. [CrossRef]
16. Trenberth, K.E.; Branstator, G.W.; Karoly, D.; Kumar, A.; Lau, N.C.; Ropelewski, C. Progress during TOGA in Understanding and Modeling Global Teleconnections Associated with Tropical Sea Surface Temperatures. *J. Geophys. Res. Ocean.* **1998**, *103*, 14291–14324. [CrossRef]
17. Mijares-Fajardo, R.; Lobato-Sánchez, R.; Patiño-Gómez, C.; Guevara-Polo, D.E. Atlantic and Pacific Sea Surface Temperature Correlations with Precipitation over Northern Mexico. *Atmosfera* **2024**, *38*, 217–234. [CrossRef]
18. Mcphaden, M.J.; Zebiak, S.E.; Glantz, M.H. ENSO as an Integrating Concept in Earth Science. *Science* **2006**, *314*, 1740–1745. [CrossRef] [PubMed]

19. Mukherjee, S.; Pal, J.; Manna, S.; Saha, A.; Das, D. El-Niño Southern Oscillation and Its Effects. In *Visualization Techniques for Climate Change with Machine Learning and Artificial Intelligence*; Elsevier: Amsterdam, The Netherlands, 2022; Volume 314, pp. 207–228.
20. Serykh, I.V.; Sonechkin, D.M. El Niño–Global Atmospheric Oscillation as the Main Mode of Interannual Climate Variability. *Atmosphere* **2021**, *12*, 1443. [CrossRef]
21. Stahle, D.W.; Cook, E.R.; Burnette, D.J.; Villanueva, J.; Cerano, J.; Burns, J.N.; Griffin, D.; Cook, B.I.; Acuña, R.; Torbenson, M.C.A.; et al. The Mexican Drought Atlas: Tree-Ring Reconstructions of the Soil Moisture Balance during the Late Pre-Hispanic, Colonial, and Modern Eras. *Quat. Sci. Rev.* **2016**, *149*, 34–60. [CrossRef]
22. Humphries, M.; Prior, K.; Green, A.; Vaughn, D. A 6000-Year High-Resolution Composite Record of El Niño-Related Drought in Subtropical Southeast Africa. *Quat. Sci. Rev.* **2024**, *344*, 108992. [CrossRef]
23. Herrera-Pantoja, M.; Hiscock, K.M. Projected Impacts of Climate Change on Water Availability Indicators in a Semi-Arid Region of Central Mexico. *Environ. Sci. Policy* **2015**, *54*, 81–89. [CrossRef]
24. Quesada-Hernández, L.E.; Calvo-Solano, O.D.; Hidalgo, H.G.; Pérez-Briceño, P.M.; Alfaro, E.J. Dynamical Delimitation of the Central American Dry Corridor (CADC) Using Drought Indices and Aridity Values. *Prog. Phys. Geogr.* **2019**, *43*, 627–642. [CrossRef]
25. UNEP. *World Atlas of Desertification*; United Nations Environment Programme: Nairobi, Kenya, 1992.
26. De Martonne, E. Une Nouvelle Function Climatologique: L'indice d'aridité [A New Climatological Function: The Aridity Index]. *La Meteorol.* **1926**, *2*, 449–458.
27. Mckee, T.B.; Doesken, N.J.; Kleist, J. The Relationship of Drought Frequency and Duration to Time Scales. In Proceedings of the 8th Conference on Applied Climatology, Anaheim, CA, USA, 17–22 January 1993.
28. Vicente-Serrano, S.M.; Chura, O.; López-Moreno, J.I.; Azorin-Molina, C.; Sanchez-Lorenzo, A.; Aguilar, E.; Moran-Tejeda, E.; Trujillo, F.; Martínez, R.; Nieto, J.J. Spatio-Temporal Variability of Droughts in Bolivia: 1955-2012. *Int. J. Climatol.* **2015**, *35*, 3024–3040. [CrossRef]
29. Palmer, W. *Meteorological Drought*; Research Paper No. 45; U.S. Weather Bureau: Silver Spring, MD, USA, 1965.
30. Corcobado, T.; Miranda-Torres, J.J.; Martín-García, J.; Jung, T.; Solla, A. Early Survival of Quercus Ilex Subspecies from Different Populations after Infections and Co-Infections by Multiple Phytophthora Species. *Plant Pathol.* **2017**, *66*, 792–804. [CrossRef]
31. Traore, V.B.; Ndiaye, M.L.; Ndiaye, R.M.; Diallo, S.; Koita, M.N.; Diaw, A.T.; Chedikh Beye, A. Spatialization of the Climate Using Aridity Indices: Case of Agro Ecological Zone of Peanut Basin, Senegal. *J. Mater. Environ. Sci.* **2020**, *11*, 2106–2122.
32. Hernández Cerda, M.E.; De Jesús Ordoñez Díaz, M.; Giménez de Azcárate, J. Comparative Analysis of Two Bioclimatic Classification Systems Applied in Mexico. *Investig. Geogr.* **2018**, *95*, 57451. [CrossRef]
33. Neira, H. *Evaluación de Los Índices de Aridez Para Colombia*; Ghent University. Master's Thesis, Ghent University, Ghent, Belgium, 2006.
34. García, E. *Modificaciones al Sistema de Clasificación Climática de Koppen*; Universidad Nacional Autónoma de México, Instituto de Geografía: Mexico City, Mexico, 1964.
35. Instituto Nacional de Estadística, Geografia e Informatica. *Guía Para La Interpretación de Cartografía Climatológica*; Instituto Nacional de Estadística, Geografia e Informatica: Aguascalientes, México, 2005.
36. INECC. *Atlas Nacional de Vulnerabilidad al Cambio Climático*, 1st ed.; Instituto Nacional de Ecología y Cambio Climático: Mexico City, México, 2019.
37. Mihai, G.; Alexandru, A.M.; Nita, I.A.; Birsan, M.V. Climate Change in the Provenance Regions of Romania over the Last 70 Years: Implications for Forest Management. *Forests* **2022**, *13*, 1203. [CrossRef]
38. Bursać, N.M.; Stričević, L.; Gocić, M. Impact of Climate Change on Agricultural Production and Agroclimatic Conditions in the Pirot Valley. *Econ. Themes* **2024**, *62*, 293–315. [CrossRef]
39. Alawadi, W.; Hassan, A.A.; Dakhil, A. Evaluation of Grid-Based Aridity Indices in Classifying Aridity Zones in Iraq. *Nat. Environ. Pollut. Technol.* **2024**, *23*, 1151–1160. [CrossRef]
40. Nistor, M.M.; Rai, P.K.; Dugesar, V.; Mishra, V.N.; Singh, P.; Arora, A.; Kumra, V.K.; Carebia, I.A. Climate Change Effect on Water Resources in Varanasi District, India. *Meteorol. Appl.* **2020**, *27*, e1863. [CrossRef]
41. Quan, C.; Han, S.; Utescher, T.; Zhang, C.; Liu, Y.S.C. Validation of Temperature-Precipitation Based Aridity Index: Paleoclimatic Implications. *Palaeogeogr. Palaeoclimatol. Palaeoecol.* **2013**, *386*, 86–95. [CrossRef]
42. Chai, R.; Mao, J.; Chen, H.; Wang, Y.; Shi, X.; Jin, M.; Zhao, T.; Hoffman, F.M.; Ricciuto, D.M.; Wullschleger, S.D. Human-Caused Long-Term Changes in Global Aridity. *npj Clim. Atmos. Sci.* **2021**, *4*, 65. [CrossRef]
43. Monterroso-Rivas, I.A.; Gómez-Díaz, D.J.; Lechuga Gayosso, M.L. Delimitación de Zonas de Influencia de Precipitación Para México. In Proceedings of the IX Congreso de la Asociación Española de Climatología, Almería, Spain, 28–30 October 2014.
44. INEGI. *Carta de Uso de Suelo y Vegetación, Serie VII, Escala 1:250000*; INEGI: Aguascalientes, Mexico, 2021.
45. CONAZA-UACh. *Informe Nacional 2022 de Acciones Contra La Desertificación, Degradación de Tierras y Sequía En México*; Comisión Nacional de Zonas Áridas: Saltillo, Mexico, 2023.

46. Fick, S.E.; Hijmans, R.J. WorldClim 2: New 1-Km Spatial Resolution Climate Surfaces for Global Land Areas. *Int. J. Climatol.* **2017**, *37*, 4302–4315. [CrossRef]
47. Trenberth, K.E. The Definition of El Nino. *Bull. Am. Meteorol. Soc.* **1997**, *78*, 2771–2778. [CrossRef]
48. National Oceanic and Atmospheric Administration Climate Prediction Center. Available online: https://www.cpc.ncep.noaa.gov/products/analysis_monitoring/ensostuff/ONI_v5.php (accessed on 30 November 2024).
49. IPCC. *Climate Change 2022: Impacts, Adaptation and Vulnerability*; Contribution of Working Group II to the Sixth Assessment Report of the Intergovernmental Panel on Climate Change; IPCC: Geneva, Switzerland, 2022.
50. Zhao, W.; Liu, L.; Shen, Q.; Yang, J.; Han, X.; Tian, F.; Wu, J. Effects of Water Stress on Photosynthesis, Yield, and Water Use Efficiency in Winter Wheat. *Water* **2020**, *12*, 2127. [CrossRef]
51. R Core Team. *R: A Language and Environment for Statistical Computing*; R Foundation for Statistical Computing: Vienna, Austria, 2025.
52. Yu, Y.; Xiao, Z.; Bruzzone, L.; Deng, H. Mapping and Analyzing the Spatiotemporal Patterns and Drivers of Multiple Ecosystem Services: A Case Study in the Yangtze and Yellow River Basins. *Remote Sens.* **2024**, *16*, 411. [CrossRef]
53. Hamed, K.H.; Rao, A.R. Hydrology A Modified Mann-Kendall Trend Test for Autocorrelated Data. *J. Hydrol.* **1998**, *204*, 182–196. [CrossRef]
54. Danneberg, J. Changes in Runoff Time Series in Thuringia, Germany-Mann-Kendall Trend Test and Extreme Value Analysis. *Adv. Geosci.* **2012**, *31*, 49–56. [CrossRef]
55. Liu, S.; Xie, Y.; Fang, H.; Du, H.; Xu, P. Trend Test for Hydrological and Climatic Time Series Considering the Interaction of Trend and Autocorrelations. *Water* **2022**, *14*, 3006. [CrossRef]
56. UACh-CONAZA. *Escenarios Climatológicos de La República Mexicana Ante El Cambio Climático*; Monterroso-Rivas, A.I., Gómez-Díaz, J.D., Eds.; UACh-CONAZA: Coahuila, Mexico, 2003.
57. PNUD-INECC. *Evaluación de Los Impactos Potenciales Sobre Los Suelos de México Ante Proyecciones de Cambio Global de 1.5 °C*; Monterroso-Rivas, A., Ed.; Elaborado en el Marco del Proyecto #86487 "Plataforma de Colaboración Sobre Cambio Climático y Crecimiento Verde entre Canadá y México"; PNUD-INECC: Mexico City, Mexico, 2017.
58. Pérez-Aguilar, L.Y.; López-Osorio, R.F.; Zambrano-Medina, Y.G.; Avila-aceves, E.; Quintero-Morales, M.A.; Monjardin-Armenta, S.A. Analysis of the Evolution of the Aridity Index in Mexico Using Geographic Information Technologies. *Georeview* **2025**, *35*, 68–87. [CrossRef]
59. Díaz-Padilla, G.; Sánchez-Cohen, I.; Guajardo-Panes, R.A.; Del Ángel-Pérez, A.L.; Ruíz-Corral, A.; Medina-García, G.; Ibarra-Castillo, D. Mapeo Del Índice de Aridez y Su Distribución Poblacional En México. *Rev. Chapingo Ser. Cienc. For. Y Del Ambiente* **2011**, *XVII*, 267–275. [CrossRef]
60. García, E.; Vidal, R.; Hernandez, M.E. Aspectos Climáticos de Las Zonas Áridas Del Norte de La Altiplanicie Mexicana. *Investig. Geogr.* **1985**, *15*, 41–74. [CrossRef]
61. López Osorio, R.F.; Pérez Aguilar, L.Y.; Zambrano Medina, Y.G.; Ávila Aceves, E. Aplicación de Evaluación Multicriterio Para Modelar Factores Climáticos y Ambientales En La Identificación de Regiones Áridas En El Noroeste de México. *Rev. Investig. En Tecnol. Inf.* **2024**, *12*, 54–70. [CrossRef]
62. Bravo-Cabrera, J.L.; Azpra-Romero, E.; Zarraluqui-Such, V.; Gay-García, C. Effects of El Niño in Mexico during Rainy and Dry Seasons: An Extended Treatment. *Atmosfera* **2017**, *30*, 221–232. [CrossRef]
63. Cabrera, J.L.B.; Romero, E.A.; Gonzalez, F.J.R.; López, O.R. Effects of ENSO on Precipitation in Mexico City. *Investig. Geogr.* **2018**, *97*, 1–12. [CrossRef]
64. Moura, M.M.; dos Santos, A.R.; Pezzopane, J.E.M.; Alexandre, R.S.; da Silva, S.F.; Pimentel, S.M.; de Andrade, M.S.S.; Silva, F.G.R.; Branco, E.R.F.; Moreira, T.R.; et al. Relation of El Niño and La Niña Phenomena to Precipitation, Evapotranspiration and Temperature in the Amazon Basin. *Sci. Total Environ.* **2019**, *651*, 1639–1651. [CrossRef]
65. Magaña, V.; Amador, J.A.; Medina, S. The Midsummer Drought over Mexico and Central America. *Am. Meteorol. Soc.* **1999**, *12*, 1577–1588. [CrossRef]
66. Karnauskas, K.B.; Seager, R.; Giannini, A.; Busalacchi, A.J. A Simple Mechanism for the Climatological Midsummer Drought along the Acic Coast of Entral America. *Atmosfera* **2013**, *26*, 261–281. [CrossRef]
67. Romero-Centeno, R.; Zavala-Hidalgo, J.; Gallegos, A.; O'brien, J.J. Isthmus of Tehuantepec Wind Climatology and ENSO Signal. *Am. Meteorol. Soc.* **2003**, *16*, 2628–2639. [CrossRef]
68. Vega-Camarena, J.P.; Brito-Castillo, L.; Farfán, L.M. Precipitation in Northwestern Mexico: Daily Extreme Events. *Theor. Appl. Climatol.* **2024**, *155*, 2689–2703. [CrossRef]
69. Zermeño-Díaz, D.M.; Gómez-Mendoza, L. The Influence of ENSO during Spring over Northwestern Mexico. *Int. J. Climatol.* **2023**, *43*, 6420–6433. [CrossRef]
70. Rohli, R.V.; Snedden, G.A.; Martin, E.R.; DeLong, K.L. Impacts of Ocean-Atmosphere Teleconnection Patterns on the South-Central United States. *Front. Earth Sci.* **2022**, *10*, 934654. [CrossRef]

71. Perdigón-Morales, J.; Romero-Centeno, R.; Ordoñez, P.; Nieto, R.; Gimeno, L.; Barrett, B.S. Influence of the Madden-Julian Oscillation on Moisture Transport by the Caribbean Low Level Jet during the Midsummer Drought in Mexico. *Atmos. Res.* **2021**, *248*, 105243. [CrossRef]
72. Huang, L.; He, B.; Chen, A.; Wang, H.; Liu, J.; Lu, A.; Chen, Z. Drought Dominates the Interannual Variability in Global Terrestrial Net Primary Production by Controlling Semi-Arid Ecosystems. *Sci. Rep.* **2016**, *6*, 24639. [CrossRef]
73. Vega-Camarena, J.P.; Brito-Castillo, L.; Pineda-Martínez, L.F.; Farfán, L.M. ENSO Impact on Summer Precipitation and Moisture Fluxes over the Mexican Altiplano. *J. Mar. Sci. Eng.* **2023**, *11*, 1083. [CrossRef]
74. Mavromatis, T.; Jagtap, S.; Jones, J. ENSO Effects on Peanut Yield and Nitrogen Leaching. *J. Clim. Res.* **2001**, *22*, 129–140. [CrossRef]
75. Lluch-Cota, S.E.; Velázquez Zapata, J.A.; Nieto Delgado, C. Agricultura, Agua y Cambio Climático En Zonas Áridas de México. *Recur. Nat. Y Soc.* **2022**, *8*, 35–48. [CrossRef]
76. López-Teloxa, L.C.; Monterroso-Rivas, A.I. Soil Organic Carbon May Decline Under Climate Change: A Case Study in Mexican Forests. *Land* **2024**, *13*, 1711. [CrossRef]
77. Herbert, E.R.; Boon, P.; Burgin, A.J.; Neubauer, S.C.; Franklin, R.B.; Ardon, M.; Hopfensperger, K.N.; Lamers, L.P.M.; Gell, P.; Langley, J.A. A Global Perspective on Wetland Salinization: Ecological Consequences of a Growing Threat to Freshwater Wetlands. *Ecosphere* **2015**, *6*, 206. [CrossRef]
78. Middleton, B.A.; Boudell, J. Salinification of Coastal Wetlands and Freshwater Management to Support Resilience. *Ecosyst. Health Sustain.* **2023**, *9*, 0083. [CrossRef]
79. Adame, M.F.; Kauffman, J.B.; Medina, I.; Gamboa, J.N.; Torres, O.; Caamal, J.P.; Reza, M.; Herrera-Silveira, J.A. Carbon Stocks of Tropical Coastal Wetlands within the Karstic Landscape of the Mexican Caribbean. *PLoS ONE* **2013**, *8*, e56569. [CrossRef]
80. Chang, S.; Gao, X.; Li, J.; Li, Q.; Song, X.; Yan, A.; Lo, K. Ecosystem Stability Assessment under Hydroclimatic Anomalies in the Arid Region of Northwest China. *Ecol. Indic.* **2024**, *169*, 112831. [CrossRef]

Disclaimer/Publisher's Note: The statements, opinions and data contained in all publications are solely those of the individual author(s) and contributor(s) and not of MDPI and/or the editor(s). MDPI and/or the editor(s) disclaim responsibility for any injury to people or property resulting from any ideas, methods, instructions or products referred to in the content.